Spatially Resolved Thermodynamics of the Partially Ionized Exciton Gas in GaAs

S. Bieker, T. Henn, T. Kiessling,* W. Ossau, and L. W. Molenkamp
Physikalisches Institut (EP3) der Universität Würzburg, 97074 Würzburg, Germany
(Received 6 February 2015; published 5 June 2015)

We report on the observation of macroscopic free exciton photoluminescence (PL) rings that appear in spatially resolved PL images obtained on a high purity GaAs sample. We demonstrate that a spatial temperature gradient in the photocarrier system, which is due to nonresonant optical excitation, locally modifies the population balance between free excitons and the uncorrelated electron-hole plasma described by the Saha equation and accounts for the experimentally observed nontrivial PL profiles. The exciton ring formation is a particularly instructive manifestation of the spatially dependent thermodynamics of a partially ionized exciton gas in a bulk semiconductor.

DOI: 10.1103/PhysRevLett.114.227402 PACS numbers: 78.55.Cr, 71.35.-y, 78.20.-e

Photocarrier excitation and excess energy relaxation, exciton formation, the related exciton electron-hole plasma (EHP) interconversion, and radiative recombination are cornerstones of semiconductor optical spectroscopy that have been investigated intensively for decades. A particular wealth of interesting phenomena arises when optical excitation by a focused laser is combined with spatially resolved photoluminescence (SRPL) detection to obtain insight into photocarrier transport processes. The observed SRPL patterns result from the intricate interplay of the above processes and the spatial diffusion of the different carrier species and are therefore often nontrivial. An example of such nontrivial SRPL patterns that currently attracts particularly strong interest is luminescence rings from indirect excitons in coupled quantum wells, which are studied intensively in the search for excitonic Bose-Einstein condensation [1,2].

In this Letter we report on the observation of macroscopic SRPL rings of free excitons in ultrapure bulk GaAs at low lattice temperatures. The excitonic rings are not related to Bose-Einstein condensation, but are rather a direct manifestation of local shifts in the thermodynamic equilibrium between Coulomb-bound free excitons and the EHP caused by optically induced temperature gradients in the carrier system. For moderate nonresonant optical excitation, a localized overheating of the carriers with respect to the crystal lattice quenches the exciton density close to the excitation spot, where consequently the uncorrelated EHP is thermodynamically favored. Interestingly, an increase in excitation density, which further raises the peak carrier temperature, can nevertheless stabilize the excitons at the laser spot.

We quantitatively model the measured exciton SRPL profiles using the Saha equation, which allows us to calculate the local ionization degree of the exciton gas from the total photocarrier density and exciton temperature profiles. An analysis of the line shape of the second LO phonon replica of the free exciton transition in our bulk sample provides direct experimental access to the exciton temperature profiles, which was not available in previous related works on coupled quantum wells [3–5]. Our analysis yields particularly instructive insights into the spatially resolved thermodynamics of the partially ionized exciton gas. It thereby extends previous works [6,7] that investigate the thermodynamics of exciton EHP interconversion in the time domain.

All data presented in this Letter are obtained on a nominally undoped, 1.5 μm thick epilayer of (001)-oriented MBE-grown GaAs. The active layer is sandwiched between two 250 (80) period $GaAs/Al_{0.09}Ga_{0.91}As$ superlattices to prevent optically excited excitons from diffusing out of the layer and to suppress surface recombination [8]. The thicknesses of the superlattices are $\approx$3 and 1 μm, respectively. The low-temperature photoluminescence (PL) spectrum of the sample (cf. Fig. 1) is dominated by the free exciton recombination line (FX), which demonstrates the high quality of the active GaAs epilayer with a negligible density of impurity atoms [9]. From a comparison with spectra reported in the literature [10,11], we estimate a residual impurity concentration of $\lesssim 1 \times 10^{12}$ cm^{-2}.

The sample is mounted on the cold finger of a helium flow optical cryostat equipped with a calibrated Cernox temperature sensor placed next to the sample. Tunable optical excitation is provided by a continuous wave Ti: sapphire laser. The laser beam is focused at normal incidence on the sample surface by an infinity-corrected NA = 0.4 microscope objective to a $(1/e)$ spot diameter of 3.6 μm. Luminescence is collected in a confocal geometry, focused on the entrance slit of a 1 m focal length monochromator equipped with a 1200 mm^{-1} grating, and detected by a liquid nitrogen cooled CCD array. Spatial information on the local PL intensity is contained in the vertical pixel number of the two-dimensional CCD image.

We show in Fig. 1 a compilation of SRPL images obtained under focused laser excitation for different sample

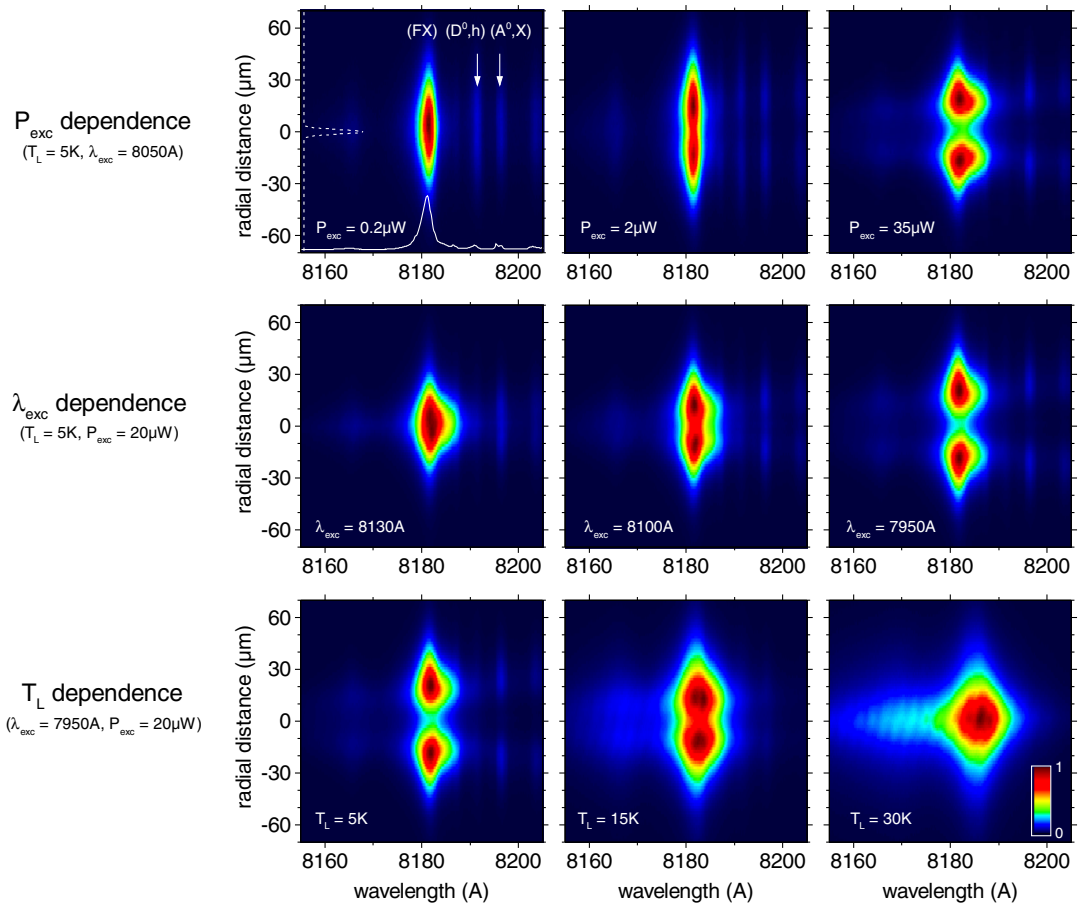

FIG. 1 (color online). Compilation of SRPL images revealing the dependence of the free exciton ring formation on various experimental parameters. Ring formation only occurs for such excitation conditions that favor the buildup of a spatial temperature gradient in the photocarrier system, i.e., low lattice temperatures, high excitation densities, and nonresonant optical excitation. In each row of SRPL images, only one parameter (indicated by the white text label) is varied while the other two parameters are kept fixed. The spatial extent of the excitation spot is the same for all measurements and is exemplarily indicated in the first panel by the dashed profile. We also show a representative low-power PL spectrum of the high-purity GaAs epilayer. Text labels indicate the usual assignment of free and bound exciton transitions [12].

temperatures T_L, excitation wavelengths λ_{exc}, and pump powers P_{exc}. For all excitation conditions, luminescence is detected at large distances ($\gtrsim 40\ \mu$m) from the excitation spot, indicating extensive spatial diffusion of the photoexcited excitons prior to their radiative recombination. Depending on T_L and optical excitation conditions, we observe a pronounced quench of the exciton luminescence intensity at the excitation center. We show in the following that this excitonic ring formation is caused by a local overheating of the photocarrier system with respect to the crystal lattice.

In a typical PL experiment, nonresonant optical excitation creates an ensemble of initially hot charge carriers and excitons, whose excess energy relaxation proceeds by emission of optical and acoustic phonons [13–15]. The limited efficiency of especially the acoustic phonon processes, however, does often not allow for a full thermalization of the photocarrier population with the crystal lattice on the time scale of its radiative lifetime. This incomplete excess energy dissipation leads therefore in a SRPL experiment with focused laser excitation to the formation of temperature gradients in the photocarrier system, which can persist over macroscopic distances [16,17].

To support our interpretation that an overheating is the mechanism underlying the free exciton ring formation, we first discuss the qualitative dependence of the local PL quench on various experimental parameters. We then present a model that provides a quantitative description of the spatially resolved (FX) PL profiles.

The excitation density dependence of the ring formation effect is summarized in the first row of the set of SRPL images presented in Fig. 1. At fixed nonresonant λ_{exc} and moderate excitation densities, the PL quench increases monotonically with P_{exc} and disappears in the low-excitation limit [18]. The ring formation also exhibits a distinct dependence on excitation wavelength λ_{exc} (second column in Fig. 1). The PL quench at the center of excitation increases for increasing photon energies. At near-resonant

optical excitation ($\lambda_{\mathrm{exc}} = 8130$ Å), i.e., when photocarriers are excited with only small amounts of excess energy, the ring formation effect disappears. Furthermore, the ring formation is most pronounced at low sample temperatures. For $T_L \gtrsim 25$ K, the cooling rate of the initially hot photocarrier ensemble increases drastically due to the availability of rapid LO phonon emission as an efficient channel of excess energy dissipation [13,15]. Irrespective of excitation wavelength and pump power, the photocarriers are in thermal equilibrium with the crystal lattice at these sample temperatures and consistently no exciton ring formation is observed at $T_L = 30$ K.

This distinct dependence on excitation power, excitation wavelength, and lattice temperature is characteristic of heating effects in the photocarrier system [15,19,20]. We therefore conclude that the free exciton ring formation is caused by a spatial exciton temperature gradient caused by the localized overheating of the carriers close to the excitation center.

The temperature of a photocarrier ensemble crucially influences the population balance between free excitons and unbound charge carriers, which is described by the Saha equation [21,22]

$$\frac{n_e n_h}{n_X} = \left(\frac{k_B T_X}{2\pi\hbar^2}\right)^{3/2} \left(\frac{m_e m_h}{m_X}\right)^{3/2} \exp\left(-\frac{E_B}{k_B T_X}\right) \quad (1)$$

with n_e, n_h, n_X the electron, hole, and free exciton densities. m_e, m_h, and m_X are the electron, hole, and exciton effective masses [23], k_B is the Boltzmann constant, $\hbar$ is the reduced Planck constant, T_X is the photocarrier temperature [24], and $E_B = 4.2$ meV is the exciton binding energy in bulk GaAs [12]. With the substitutions $n_X = f_X n_0$ and $n_e = n_h = (1 - f_X) n_0$, we can compute from the Saha equation the relative fraction f_X of free excitons among a photocarrier population of density n_0 at a given temperature T_X.

The contour plot $f_X(n_0, T_X)$ in Fig. 2 reveals two general trends that characterize the thermodynamics of a partially ionized exciton gas in a semiconductor. Thermal breakup of Coulomb-bound excitons at increased temperatures T_X shifts the population balance towards the uncorrelated EHP. At fixed T_X, an increase of the total photocarrier density n_0, however, leads to a relative increase of the free exciton population. The temperature and density dependent population balance is crucial for a quantitative understanding of the free exciton ring formation effect.

Our model description of the spatially dependent ionization degree of the exciton gas assumes the following physical picture. Under nonresonant focused laser excitation, lateral photocarrier diffusion [27] leads to the formation of a radially symmetric total photocarrier density profile $n_0(r)$ and spatial temperature gradient $T_X(r)$. At each distance r from the excitation spot, the local free exciton density $n_X(r)$ is then given by the product

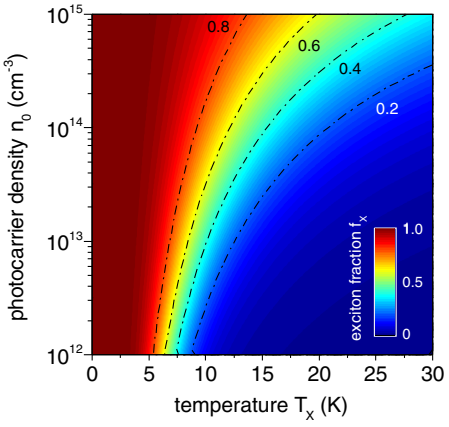

FIG. 2 (color online). Contour plot of the temperature and density dependent population balance between free excitons and the EHP described by the Saha equation. Color indicates the relative fraction $f_X = n_X/n_0$ of free excitons among the entire photocarrier population of density n_0. Free excitons are stabilized against thermal breakup into unbound charge carriers by an increase of the total photocarrier density.

$$n_X(r) = n_0(r) \times f_X[n_0(r), T_X(r)]. \quad (2)$$

In a ring formation scenario, the missing free excitons at the excitation center are converted into unbound charge carriers by the localized overheating.

We first consider the temperature profile $T_X(r)$. The nontrivial line shape of the free exciton luminescence in a bulk semiconductor [28,29] impedes a direct determination of the exciton temperature T_X from the zero-phonon line (FX). The low defect concentration in our sample, however, allows for the detection of the second LO phonon replica of the free exciton transition $(FX) - 2\hbar\Omega_{\mathrm{LO}}$, which is known to reflect the density of occupied states among the thermalized free exciton ensemble [30,31]. We therefore directly obtain the exciton temperature profile $T_X(r)$ from a spatially resolved Maxwellian line shape analysis of the $(FX) - 2\hbar\Omega_{\mathrm{LO}}$ transition. A representative fit to the second LO phonon replica and a set of resulting $T_X(r)$ profiles for three exemplary excitation powers P_{exc} is shown in Figs. 3(a)–3(c) and 3(g). We indeed observe a significant overheating of the photoinduced exciton population, peaked at the center of the excitation spot. Moreover, we find that hot excitons are present for distances that significantly exceed the spatial extent of the excitation spot, indicating that heat transport takes place in the carrier system. Even far away from the laser spot ($r \gtrsim 40$ μm) the excitons have not thermalized with the lattice. The increased base temperature of the $T_X(r)$ profiles with respect to T_L is a consequence of the competing time scales of excess energy dissipation by phonon emission and the lifetime of the excitons; i.e., excitons (and free carriers) on average recombine before dissipating their total excess energy [17].

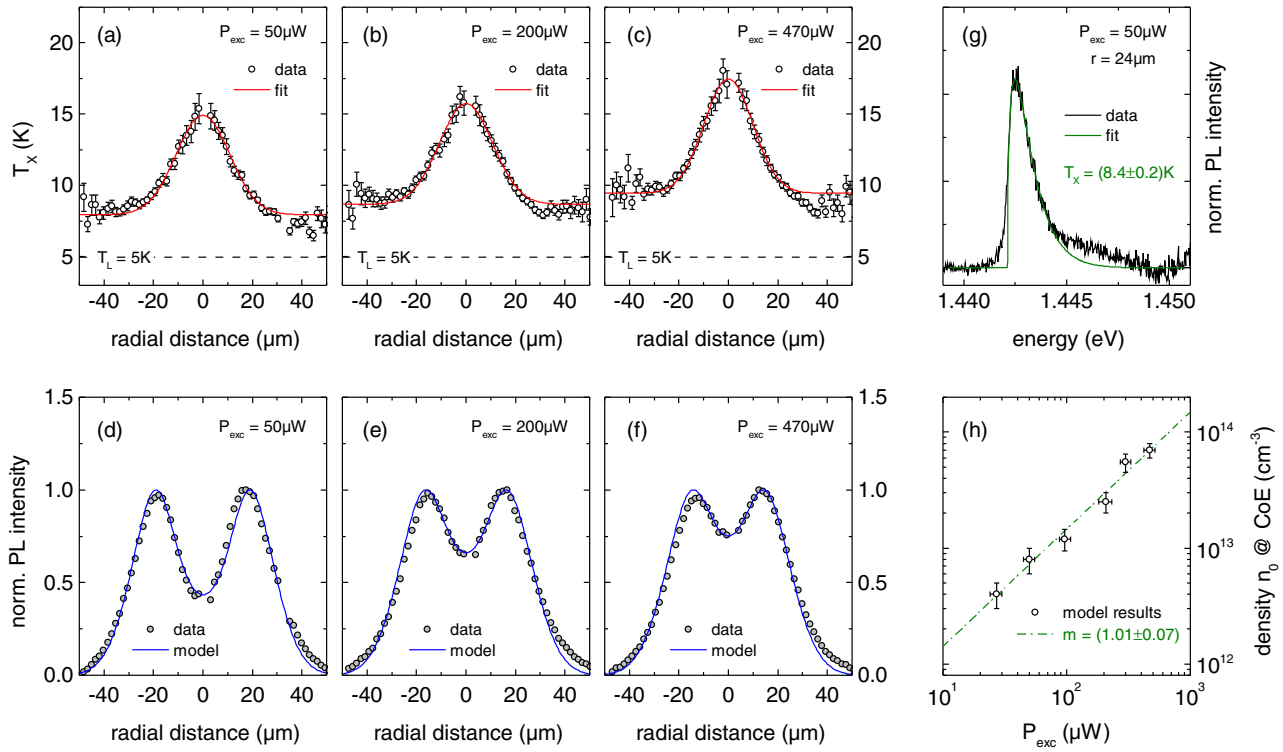

FIG. 3 (color online). Model description of the free exciton ring formation effect. All measurements are performed at $\lambda_{\mathrm{exc}} = 8050$ Å. (a)–(c) Exciton temperature profiles $T_X(r)$ as obtained from spatially resolved Maxwellian line shape analyses of the $(FX) - 2\hbar\Omega_{\mathrm{LO}}$ transition. (d)–(f) Data points show the spectrally integrated PL intensity of the second LO phonon replica; solid blue lines indicate our model results for the free exciton density profiles $n_X(r)$. (g) Representative line shape analysis of the $(FX) - 2\hbar\Omega_{\mathrm{LO}}$ replica to determine the exciton temperature T_X. (h) The peak total photocarrier density $n_0(r = 0)$ at the center of excitation (CoE) obtained from our model analysis scales linearly with the optical excitation power P_{exc}.

Because of K vector conservation, only a subset of the entire free exciton population near the Brillouin zone center at $K \approx 0$ can recombine radiatively and contribute to the PL intensity of the free exciton zero-phonon line [9,14]. The (FX) SRPL profile is therefore not a direct measure for the local free exciton density in the crystal. The K vector selection rule, which applies to the zero-phonon line, however, is fully relaxed for the radiative recombination of free excitons under simultaneous emission of two LO phonons [30,31]. Undistorted $n_X(r)$ profiles are therefore obtained from the spectrally integrated SRPL intensities of the $(FX) - 2\hbar\Omega_{\mathrm{LO}}$ replica [32], indicated by the data points in Figs. 3(d)–3(f).

We assume a Gaussian profile with 55 μm $(1/e)$ full width as a first approximation for the combined total carrier density diffusion profile $n_0(r)$ in our model. The Gaussian profile is adjusted to the wings $|r| \gtrsim 25$ μm of the $(FX) - 2\hbar\Omega_{\mathrm{LO}}$ SRPL profile where the base temperature of the $T_X(r)$ profile is reached and where consequently the undistorted $n_0(r)$ is observed. The width of the diffusion profile is assumed to not depend on pump power. The total photocarrier density $n_0(r = 0)$ at the center of optical excitation then remains the only variable model parameter.

As demonstrated in Figs. 3(d)–3(f), excellent agreement of the calculated free exciton density profile $n_X(r)$ with the $(FX) - 2\hbar\Omega_{\mathrm{LO}}$ SRPL data is obtained for all excitation densities by only adjusting the peak photocarrier density $n_0(r = 0)$. This peak density scales linearly with optical excitation power P_{exc} [Fig. 3(h)], which we regard as strong evidence that our model captures the essential physics underlying the (FX) ring formation effect.

Our model furthermore provides a very natural explanation for an initially counterintuitive trend observed in the experiment. The peak amplitude of the $T_X(r)$ profile increases monotonically with P_{exc} [Figs. 3(a)–3(c)] and one might therefore expect the most pronounced quench of the PL intensity at the highest excitation densities. The stabilizing effect of an increased total photocarrier density n_0 (Fig. 2), however, overcompensates further thermal breakup of free excitons at the excitation spot and leads to a less pronounced local quench of the free exciton density $n_X(r = 0)$ in the high excitation limit.

To summarize, we have observed the ring formation of free excitons in ultrapure bulk GaAs. The dependence of the (FX) SRPL patterns on various experimental parameters is a particularly instructive example for the spatially resolved thermodynamics of a partially ionized exciton gas in a semiconductor. The temperature and density dependent population balance between free excitons and the EHP naturally explains the observation of macroscopic free

exciton ring structures in our SRPL experiment. Combined with exciton temperature profiles, which we directly obtain from the $(FX) - 2\hbar\Omega_{\mathrm{LO}}$ phonon replica, the Saha equation allows for a quantitative modeling of the local thermodynamics of an exciton gas in a bulk semiconductor.

The authors gratefully acknowledge financial support by the DFG (SPP1285 OS98/9-3). The excellent GaAs sample was grown at Philips Research Laboratories, Redhill, UK by J. J. Harris and C. T. Foxon.

*tobias.kiessling@physik.uni-wuerzburg.de

[1] L. V. Butov, A. C. Gossard, and D. S. Chemla, Nature (London) **418**, 751 (2002).
[2] D. Snoke, S. Denev, Y. Liu, L. Pfeiffer, and K. West, Nature (London) **418**, 754 (2002).
[3] A. L. Ivanov, L. E. Smallwood, A. T. Hammack, S. Yang, L. V. Butov, and A. C. Gossard, Europhys. Lett. **73**, 920 (2006).
[4] A. T. Hammack, L. V. Butov, J. Wilkes, L. Mouchliadis, E. A. Muljarov, A. L. Ivanov, and A. C. Gossard, Phys. Rev. B **80**, 155331 (2009).
[5] J. R. Leonard, M. Remeika, M. K. Chu, Y. Y. Kuznetsova, A. A. High, L. V. Butov, J. Wilkes, M. Hanson, and A. C. Gossard, Appl. Phys. Lett. **100**, 231106 (2012).
[6] H. W. Yoon, D. R. Wake, and J. P. Wolfe, Phys. Rev. B **54**, 2763 (1996).
[7] R. A. Kaindl, D. Hägele, M. A. Carnahan, and D. S. Chemla, Phys. Rev. B **79**, 045320 (2009).
[8] R. J. Nelson and R. G. Sobers, J. Appl. Phys. **49**, 6103 (1978).
[9] G. W. 't Hooft, W. A. J. A. van der Poel, L. W. Molenkamp, and C. T. Foxon, Phys. Rev. B **35**, 8281 (1987).
[10] U. Heim and P. Hiesinger, Phys. Status Solidi B **66**, 461 (1974).
[11] J. Aaviksoo, I. Reimand, V. V. Rossin, and V. V. Travnikov, Phys. Rev. B **45**, 1473 (1992).
[12] M. R. Brozel and G. E. Stillman, *Properties of Gallium Arsenide* (INSPEC, The Institution of Electrical Engineers, London (UK), 1996).
[13] R. Ulbrich, Phys. Rev. B **8**, 5719 (1973).
[14] S. Permogorov, Phys. Status Solidi B **68**, 9 (1975).
[15] S. A. Lyon, J. Lumin. **35**, 121 (1986).
[16] T. Kiessling, J. H. Quast, A. Kreisel, T. Henn, W. Ossau, and L. W. Molenkamp, Phys. Rev. B **86**, 161201 (2012).
[17] S. Bieker, T. Henn, T. Kiessling, W. Ossau, and L. W. Molenkamp, Phys. Rev. B **90**, 201305(R) (2014).
[18] The reverse trend of the stabilization of the excitons with increasing P_{exc} observed in the high excitation limit [Figs. 3(d)–3(f)] is discussed later.
[19] J. Shah, Solid State Electron. **21**, 43 (1978).
[20] J. Shah, *Ultrafast Spectroscopy of Semiconductors and Semiconductor Nanostructures* (Springer, New York, 1999).
[21] W. D. Kraeft, K. Kilimann, and D. Kremp, Phys. Status Solidi B **72**, 461 (1975).
[22] G. Bastard, *Wave Mechanics Applied to Semiconductor Heterostructures* (Wiley, New York, 1988).
[23] $m_e = 0.067m_0$ and $m_h = 0.51m_0$ with $m_0 = 9.11 \times 10^{-31}$ kg the free electron mass and $m_X = m_e + m_h$.
[24] We assume that efficient exciton-exciton and exciton-free carrier scattering [25] maintain a thermal equilibrium among all photocarrier species, such that electrons, holes, and free excitons share the same temperature T_X [26].
[25] L. Schultheis, J. Kuhl, A. Honold, and C. W. Tu, Phys. Rev. Lett. **57**, 1635 (1986).
[26] D. Robart, X. Marie, B. Baylac, T. Amand, M. Brousseau, G. Bacquet, G. Debart, R. Planel, and J. M. Gerard, Solid State Commun. **95**, 287 (1995).
[27] The characteristic diffusion length in the investigated sample significantly exceeds the thickness of the GaAs epilayer. The photocarrier density and temperature profiles are therefore homogeneous along the sample normal and diffusion perpendicular to the sample surface can be neglected.
[28] J. Hopfield, Phys. Rev. **112**, 1555 (1958).
[29] J. Lee, E. S. Koteles, M. O. Vassell, and J. P. Salerno, J. Lumin. **34**, 63 (1985).
[30] E. Gross, S. Permogorov, and B. Razbirin, J. Phys. Chem. Solids **27**, 1647 (1966).
[31] B. Segall and G. D. Mahan, Phys. Rev. **171**, 935 (1968).
[32] For each distance r we determine the total intensity of the second LO phonon replica of the free exciton transition by spectrally integrating the area below the fit curve that results from the Maxwellian line shape analysis of the local $(FX) - 2\hbar\Omega_{\mathrm{LO}}$ luminescence spectrum.